

PAPER • OPEN ACCESS

Including installation logistics costs in the optimal sizing of semi-submersibles for floating wind farms

To cite this article: M Baudino Bessone *et al* 2022 *J. Phys.: Conf. Ser.* **2265** 042018

View the [article online](#) for updates and enhancements.

You may also like

- [Upscaling and levelized cost of energy for offshore wind turbines supported by semi-submersible floating platforms](#)

Yuka Kikuchi and Takeshi Ishihara

- [Integrated design of a semi-submersible floating vertical axis wind turbine \(VAWT\) with active blade pitch control](#)

Fons Huijs, Ebert Vlasveld, Maël Gormand et al.

- [Time-domain coupling analysis of semi-submersible floating foundation with four buoys for offshore wind turbine and its mooring system](#)

Xueping Rong, Peilin Dou and Jianxin Chen



ECS Membership = Connection

ECS membership connects you to the electrochemical community:

- Facilitate your research and discovery through ECS meetings which convene scientists from around the world;
- Access professional support through your lifetime career;
- Open up mentorship opportunities across the stages of your career;
- Build relationships that nurture partnership, teamwork—and success!

Join ECS!

Visit electrochem.org/join



Including installation logistics costs in the optimal sizing of semi-submersibles for floating wind farms

M Baudino Bessone¹, M Zaaier¹, D von Terzi¹, K Dykes², E Jump³
and A Viré¹

¹ Delft University of Technology, Kluyverweg 1, 2629HS Delft, the Netherlands

² Technical University of Denmark, Frederiksborgvej 399, 4000, Roskilde, Denmark

³ ORE Catapult, 121 George Street, Glasgow, G1 1RD, United Kingdom

E-mail: M.baudinobessone@tudelft.nl

Abstract. In this research, we explored the potential to reduce the cost of floating wind farms by adopting an integrated approach to optimally size semi-submersible substructures accounting for materials, fabrication and installation-logistics-related costs. A trade-off between manufacturing and installation costs was identified. This trade-off is driven by the growth of shipyard costs when the size of the structure increases, counteracting the reduction of fabrication costs achieved with a larger semi-submersible footprint. For the reference scenario, accounting for this trade-off yields a design that is a few tenths of a percent cheaper than when minimising only fabrication costs. However, the obtained design has a considerably smaller footprint than the fabrication-only case. The sensitivity of this trade-off to different installation strategies affecting the required storage area at the shipyard was assessed. When fabrication costs are dominant, the advantage of accounting for installation costs in the design process is negligible. Instead, larger storage area requirements increase the cost reduction achieved by optimising the semi-submersible while simultaneously accounting for fabrication and installation costs. The coupling effect remained significant for all the cases considered in a further sensitivity analysis of key parameters affecting the cost-optimal design. Furthermore, we identified several different designs that provide enough hydrostatic restoring moment in pitch to counteract the thrust-induced overturning moment within a small cost range from the most cost-effective one. This result suggests that additional criteria than minimising manufacturing and installation costs could drive the final design choice.

1. Introduction

Floating wind energy is a promising technology, as it opens the door to the exploitation of wind resource in waters deeper than 60 meters, which opens up new markets [1]. Moving to deeper waters is made possible by adopting floating substructures, whose typology often falls into the categories of spar buoy, semi-submersible, barge or tension-leg platform (TLP). However, hybrid concepts that aim to combine the strength of different substructure typologies are currently under test [2]. Among the various concepts, semi-submersibles are particularly interesting due to their relatively simple installation procedures, and the potential for offsite maintenance.

However, floating wind's Levelised Cost of Energy (LCoE) is still much higher than that of conventional offshore wind, and significant cost reductions are necessary to make floating wind a competitive technology. Different works have dealt with the optimal sizing and design of floating substructures for wind turbines, targeting materials or manufacturing costs minimisation



Content from this work may be used under the terms of the [Creative Commons Attribution 3.0 licence](https://creativecommons.org/licenses/by/3.0/). Any further distribution of this work must maintain attribution to the author(s) and the title of the work, journal citation and DOI.

[3, 4, 5, 6, 7, 8]. However, logistics, transportation, assembly, and installation costs constitute about 9% of the overall CapEx for a floating wind farm [9]. Avoiding specialised, expensive vessels and minimising time and space required at the shipyard or port can have a substantial cost reduction impact for floating wind farms [10, 11]. As installation costs may depend on floater size, they may also influence the optimal sizing of the floating substructure.

This study aims to gain insight into the potential of adopting an integrated approach to the design of floating semi-submersibles for wind turbines. To this end, this research investigates the interactions between manufacturing and installation costs, focusing on the significance of the couplings and highlighting main trends and drivers for cost reduction, rather than on the detailed design of semi-submersible support structures for floating wind turbines. With respect to previous research in this field, we optimised the sizing of a floating semi-submersible substructure for wind turbines while simultaneously considering materials, manufacturing and installation logistics-related costs. In doing so, this research steps toward reducing floating wind farms' LCoE by adopting a more comprehensive approach, from a full wind farm perspective.

2. Methodology

2.1. Semi-submersible sizing

The geometry of the semi-submersible is parametrised similarly to what was proposed in [3] and [4]. Six design variables are defined, which are represented in Figure 1 and reported together with their boundaries in Table 1. The remaining geometrical and structural design parameters

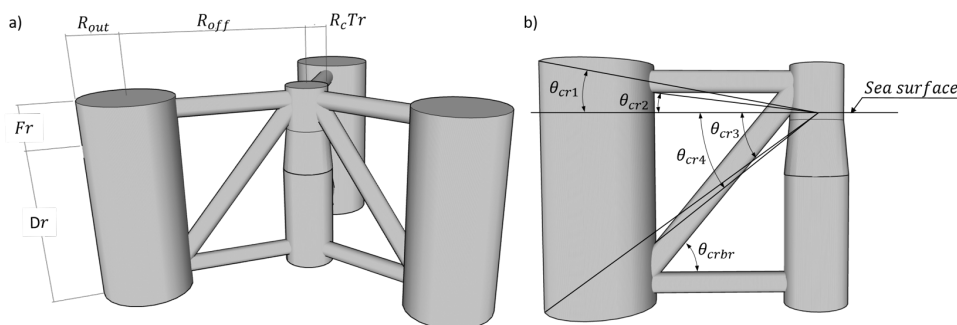


Figure 1. a) Design variables for semi-submersible sizing and b) rotation angles determining the submersion or emersion of a semi-submersible element, and cross-bracing angle, θ_{crbr}

Table 1. Semi-submersible design variables

Design variable	Adopted symbol	Boundaries
Radius of the outer columns	R_{out}	3m-8m
Radial distance between the central and outer columns	R_{off}	25m-50m
Draft between the sea surface and the keel	Dr	10m-50m
Freeboard height between the sea surface and the deck	Fr	5m- ∞
Radius of the central column at the keel	R_c	3m-8m
Taper ratio between R_c at the interface with the tower and R_c at the keel	Tr	0.5-0.95

for the semi-submersible are defined as constants or fully determined by combinations of other parameters and design variables and reported in Table 2. The structure is manufactured with steel, whose density $\rho_s = 8500 \frac{kg}{m^3}$ is set higher than the typical value to account for the added weight of welds, paint, caps, and the deck platform. The wind turbine supported by the floater is the NREL 5 MW [12] The three outer columns and the central column are filled with ballast

Table 2. Semi-submersible geometrical and structural parameters

Parameter	Adopted symbol	Parameter value
Taper angle of the tapered section of the central column	θ_{tpr}	10.3°, from the OC3 spar buoy tapered section [13]
Length below the sea surface of the section of the central column piercing the water	L_{prc}	Twice the significant wave height, H_s
Thickness of the central and outer column	th_{clm}	0.05m [3, 4]
Connection height of the cross braces with the upper section of the central column	Up_{crbr}	75% of freeboard height [14]
Connection depth of the cross braces with the lower section of the outer column	Low_{crbr}	80% of draft [14]
Diameter of cross braces, upper and lower pontoons	D_{crbr}	As in [3, 4], considering only displaced mass of water of one outer column in the definition of the critical buckling load
Cross braces and pontoons wall thickness to radius ratio	r_{th}	0.022 [14]

material, which is concrete with density $\rho_c = 2400 \frac{kg}{m^3}$. The amount of ballast is computed to ensure the neutral buoyancy of the turbine and substructure assembly. The impact of mooring lines is not considered for this preliminary study. Furthermore, it is assumed that there is no restriction on the size of the semi-submersible due to fabrication or installation requirements, further than the design variables' boundaries reported in Table 1.

2.2. Problem formulation

When only fabrication costs are considered, the optimisation problem is formulated as:

Minimise

$$M_s C_s + M_c C_c + M_s C_s MCF \quad (1)$$

Subject to

$$\rho_w g [I_{sms} + V_{sbg} (KB - KG)] \sin \theta_{pp} - T_{rtd} (HH + Fr + OB) \geq 0 \quad (2)$$

$$Dr \geq \max \left\{ \begin{array}{l} (R_{off} + R_{out}) \tan \theta_{el} \\ (1 - Low_{crbr}) Dr + \frac{D_{crbr}}{2 \cos \theta_{crbr}} + (R_{off} - R_{out}) \tan \theta_{el} \\ Low_{crbr} Dr + \frac{D_{crbr}}{2 \cos \theta_{crbr}} + D_{crbr} \end{array} \right. \quad (3a)$$

$$Dr \geq \max \left\{ \begin{array}{l} (R_{off} + R_{out}) \tan \theta_{el} \\ (1 - Low_{crbr}) Dr + \frac{D_{crbr}}{2 \cos \theta_{crbr}} + (R_{off} - R_{out}) \tan \theta_{el} \end{array} \right. \quad (3b)$$

$$Dr \geq \max \left\{ \begin{array}{l} (R_{off} + R_{out}) \tan \theta_{el} \\ Low_{crbr} Dr + \frac{D_{crbr}}{2 \cos \theta_{crbr}} + D_{crbr} \end{array} \right. \quad (3c)$$

$$Fr \geq \max \begin{cases} 2H_s & (4a) \\ (R_{off} + R_{out}) \tan \theta_{el} & (4b) \\ (1 - U_{p_{crbr}}) Fr - \frac{D_{crbr}}{2 \cos \theta_{crbr}} + (R_{off} - R_{out}) \tan \theta_{el} & (4c) \\ U_{p_{crbr}} Fr + \frac{D_{crbr}}{2 \cos \theta_{crbr}} + D_{crbr} & (4d) \end{cases}$$

$$2R_c Tr \geq D_{twrb} \quad (5)$$

The objective function accounts for the materials cost of the structure and the ballast and fabrication costs. M_s and M_c are the mass of the steel substructure and concrete ballast. Steel cost C_s and concrete cost C_c are set at $604 \frac{\text{€}}{\text{t}}$ and $86.6 \frac{\text{€}}{\text{t}}$, respectively [5]. Manufacturing costs are computed by means of a Manufacturing Complexity Factor, MCF, equal to 1.9 [5, 15].

The semi-submersible is sized so that the hydrostatic restoring moment in pitch is equal to or greater than the overturning moment resulting from the maximum thrust force acting on the turbine at rated wind speed, $T_{rtd} = 820 \text{ kN}$. This constraint is expressed by Equation (2). I_{sms} is the area moment of inertia of the semi-submersible at the warplane. KG and KB are, respectively, the vertical distance between the keel of the floater and the centre of gravity, and between the keel and the centre of buoyancy. OB is the vertical distance between the sea surface and the centre of buoyancy of the semi-submersible. V_{sbg} is the displaced volume of the substructure. $HH = 90\text{m}$ is the hub height from the turbine-substructure interface. ρ_w is the water density, $1025 \frac{\text{kg}}{\text{m}^3}$, and $g = 9.81 \frac{\text{m}}{\text{s}^2}$ is the gravitational acceleration. The maximum pitch angle allowed during power production, θ_{pp} , is set to 6° [6]. The metacentric height is computed for the undisturbed conditions, and it is not recalculated in the heeled configuration. It is assumed that the heel angles are small and that enough freeboard and draft are provided so that the metacentric height can be considered constant [6, 16]. To further support this assumption, it is ensured that the smallest angles that would determine the submersion or emersion of an element of the semi-submersible is larger than the maximum allowable heel angle, i.e. that no element emerges or is submerged at the maximum allowed heeling angle, so that the geometry remains similar within the allowable pitch range [17]. These constraints are expressed by Equations (3a) and (3b) for the minimum draft, (4b) and (4c) for the minimum freeboard. The maximum heel angle that is allowed for the extreme load case is set at $\theta_{el}=12^\circ$ [6]. Critical angles are illustrated together with the cross bracing angle θ_{crbr} , in Figure 1. Further constraints are set to provide enough draft, (3c), and freeboard, (4d), for the connection of the lower and upper pontoon to the outer and central column. Furthermore, it is enforced that the minimum freeboard height is higher than or equal to $2H_s$, to keep the semi-submersible platform away from the waves' splash zone, Equation (4a). H_s is set to 2m. Finally, it is enforced that the diameter of the central column of the semi-submersible at the interface with the tower is at least equal to the NREL 5MW tower base diameter, $D_{twrb} = 6\text{m}$.

When installation costs are taken into account, the objective of the optimisation becomes:

Minimise

$$M_s C_s + M_c C_c + M_s C_s MCF + \frac{C_{inst}}{NFU} \quad (6)$$

with C_{inst} total installation cost computed as described in Sections 2.3 and 2.4, and NFU the number of floating units for the reference farm. The constraints implemented are the same as in the case where only manufacturing costs are considered.

The optimisation workflow is set in OpenMDAO [18], adopting the Sequential Least Squares Programming algorithm (SLSQP) with an absolute tolerance of 10^{-8} .

To verify the semi-submersible sizing approach, this methodology was applied to replicate the OC4 semi-submersible geometry [14]. The lower bound of R_{out} was set to 6m, to obtain the same

size of the outer columns of the OC4 floater. The tower properties and thickness of the vertical columns were modified to match the OC4 design. The obtained geometry matched the OC4 design relatively well. The main difference was found in the steel mass and displaced water mass. These amount to 2437t and 7278t for the current design and to 3852t and 14267 for the OC4 design, respectively. This discrepancy is due to the large base columns of the OC4 structure, not considered in this work. Neglecting the base columns, the steel mass and displaced water mass of the OC4 design become 2463t and 8118t, respectively, much closer to the obtained design.

2.3. Installation procedure

To estimate the installation costs, an installation procedure reflecting the current installation methodology for semi-submersibles was defined [19, 20]. The operations are carried out around the clock. Phases (i) to (v) are assumed to be sequential, i.e. no parallelisation is considered:

- (i) The floaters are transported from the fabrication shipyard to the port. There, the turbines are assembled on the semi-submersibles. This phase involves the following sub-phases:
 - (a) Float-out from the shipyard
 - (b) Prepare the semi-submersible for towing to port
 - (c) Tow the semi-submersible to port

The installation procedure is expected to begin after fabricating the semi-submersibles at the shipyard. Semi-submersibles are anticipated to be floated out and towed to port one by one. Having secured the floater at quayside, the towing vessels are instructed to return to the shipyard to tow the subsequent structure to port.

- (ii) The assembly of the wind turbines on the semi-submersibles takes place at the quayside.
- (iii) Mechanical completion and verification of the turbine-substructure assemblies are carried out at the quayside.
- (iv) After pre-commissioning at the quayside, the turbine-substructure floating assemblies are towed to the site and installed at their pre-defined positions. This phase is composed of the following sub-phases:
 - (a) Prepare the semi-submersible for towing to site
 - (b) Tow the semi-submersible to site
 - (c) Install the floating assembly at site

The turbine-substructure assemblies are towed to the site one by one. The mooring lines and the dynamic cable are connected to the substructure at the site. Having installed one floating assembly at the site, the towing vessels are instructed to return to the port to tow the subsequent floating assembly to the installation site.

- (v) A final installation check is performed, and the floating assembly is commissioned.

2.4. Installation cost model

Installation logistics-related costs were computed by means of a deterministic cost model, based on the methodology presented in [15] and [21]. The costs incurred in the first phase of the procedure include the daily rates of one large and two small tugboats that are chartered to assist the float-out operations and tow the semi-submersible to the port, and the cost of the slipway used to float out the semi-submersibles. The float out cost is assumed to equal the cost of one quayside crane lift [15, 21]. A mobile crane is deployed at the quayside to assemble the wind turbine components for the second phase. Seven lifts are necessary to install the turbine on the substructure: three lifts for three tower sections, one lift for the pre-assembled nacelle and hub, and three lifts for the blades. The pre-commissioning phase is carried out with the aid of a small tugboat. Two anchor handling tug supply vessels (AHTS) and two small tugboats are chartered to tow the turbine-substructure assemblies to the site and assist the hook-up of the mooring

lines to the substructure. A cable laying vessel performs the connection of the dynamic cable. Commissioning at the site is aided by a small tugboat. The length of the different installation phases and costs of the vessels and port equipment are reported in Table 3.

Table 3. Logistics and vessel rates assumptions

Description	Value	Reference	Notes
Time to float-out the semi-submersible	$3h$	[21]	
Time to prepare the semi-submersible for towing operations	$2h$	[22]	Same time assumed as for the spar
Time to lift and assemble a turbine's component on the semi-submersible	$3h$	[21]	
Mechanical completion and verification of one floating unit at quayside	$24h$	[23]	
Time to install one floating unit at the site	$14h$	[15],[21], [22],[23]	Average of the different references. [22]: same time assumed as for the spar
Check installation of one floating unit at the site	$12h$	[23]	
Daily rate of a small tugboat	$4135 \frac{\text{€}}{\text{day}}$	[2], [24]	Average of the different references
Daily rate of a large tugboat	$28321 \frac{\text{€}}{\text{day}}$	[21],[24], [25]	Average of the different references
Daily rate of an AHTS	$39891 \frac{\text{€}}{\text{day}}$	[24],[25]	Average of the different references
Daily rate of a cable laying vessel	$101232 \frac{\text{€}}{\text{day}}$	[25]	
Hourly rate of a quayside crane	$833 \frac{\text{€}}{h}$	[21]	
Daily rate of storage space at shipyard or port	$0.18 \frac{\text{€}}{m^2 \text{day}}$	[26]	Converted from original weekly rate
Daily rate for a semi-submersible resting at quayside	$300 \frac{\text{€}}{\text{day}}$	[27]	Daily semi-submersible lay up anchorage tariff assumed as representative for the cost of one floater resting at quayside

The cost incurred to store the substructures at the shipyard is computed as:

$$C_{shp} = NFU A_{mf} L_{sms} W_{sms} t_{shp} C_{A,dl} \quad (7)$$

It is proportional to the rectangular footprint area identified by the length, L_{sms} , and width, W_{sms} of the semi-submersible. A_{mf} is a multiplication factor that is applied to account for extra storage space required for internal movements. The extra space is initially assumed to be equal to 10% of the storage area. The period during which the storage space is rented, t_{shp} , starts at the beginning of the installation operations and ends when the last substructure is towed from the shipyard to the port. $C_{A,dl}$ is the daily rate for storage space at the shipyard or port, reported in Table 3. The cost incurred to store the turbines' components at port,

$$C_{prt} = NFU A_{mf} [3 L_{bld} C_{bld} + 3 \frac{\pi D_{twrb}^2}{4}] t_{prt} C_{A,dl} \quad (8)$$

is proportional to the area required to store the turbine components, three blades and three tower sections. $L_{bld} = 61.5m$ is the blade length and $C_{bld} = 4.65m$ is the maximum blade chord.

An area multiplication factor is applied also in this case. The period throughout which the storage space at the port is rented, t_{prt} , starts at the beginning of the installation activities and ends when the last turbine is assembled on the semi-submersible.

Finally, the cost incurred to berth the semi-submersibles at quayside,

$$C_{qsd} = N F U t_{qsd} C_{qsd} \quad (9)$$

depends on the daily rate for one floating turbine-substructure assembly resting at the quayside, C_{qsd} , that is reported in Table 3. The period during which the quayside space is rented, t_{qsd} , starts at the beginning of the installation procedure until the last floating turbine substructure assembly is installed at the site. It is assumed that enough space is available at the shipyard and port to store the semi-submersibles and turbines' components, respectively, as well as quayside space for quayside operations. A workability factor of 50% is adopted to take into account delays due to bad weather for those operations that are carried out at sea, as a surrogate of complex installation dynamics related to the weather window [15, 21].

The installation cost model was compared with the one presented in [15, 28]. The two cost models were applied to the same scenario: installing a floating wind farm of 100 5MW units located at 200km from shore. Neglecting cost items considered only in one of the two cost models and assuming the same vessels rates, the two models yielded a very close estimation of the installation costs for the floating wind farm. The reference model estimated installation costs of $213 \frac{k\text{€}}{\text{turbine}}$, while the current cost model estimate amounted to $216 \frac{k\text{€}}{\text{turbine}}$. Despite this good likeness, the absolute values of these results have to be considered with care, as the neglected cost items can be relevant and significant.

3. Results

3.1. Case study

A case study based on a 300MW reference wind farm was defined. The farm is located 30km from the port used as the base for the installation. The distance between the port and the manufacturing shipyard is 150km. A multi-start approach was adopted to investigate the design space. The optimisation was initialised with different combinations of R_{out} and R_{off} , to cover the entire design space up to the bounds defined in Section 2.1. In particular, R_{out} varied between 3m and 8m, with 0.5m steps, while R_{off} varied between 25m and 50m, with 1m steps.

The semi-submersible was first optimised to minimise only manufacturing costs. Then, installation costs were included in the objective function. The 150 best results obtained for both cases are presented in Figure 2. It can be noticed that several quite different designs fulfil the stability constraint and are comprised within a small cost range. The 150 best designs obtained considering only fabrication costs are within 0.34% from the most cost-effective design. Instead, differences in terms of R_{out} and R_{off} are up to the 13.8% and 14.7%, respectively. For the case including installation costs, the maximum cost difference is 0.21%. The differences in R_{out} and R_{off} reach 11%, and 11.8%, respectively. These results show a nearly flat region of the objective function around the identified optimum. In this region, other criteria than minimising the fabrication and installation costs could be chosen to pick one design over the other.

Further, including installation costs into the objective function of the optimisation results in an optimum design with a lower R_{off} and a higher R_{out} than for the manufacturing-only case. This is due to a trade-off between fabrication costs and the floater's storage costs at the shipyard. Manufacturing costs are significantly reduced by lowering the amount of steel in the substructure, which is achieved by decreasing the radius of the outer columns. Concurrently, the offset between the outer and central columns is increased to fulfil the stability constraint. Instead, installation costs increase with larger R_{off} due to the increase of storage space required at the shipyard. This trade-off is illustrated in Figure 3. In this case, pairs of R_{off} and R_{out} were defined, and the remaining design variables were optimised for each identified combination. R_{off} varies between

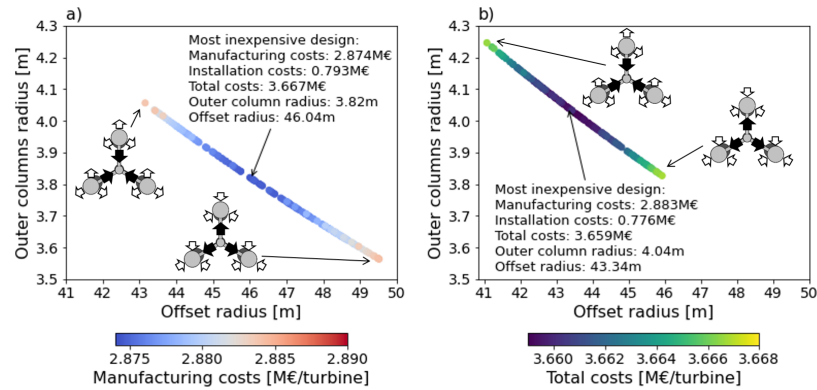


Figure 2. Cost of the 150 best semi-submersible designs obtained from the multi-start optimisations. a) objective limited to fabrication costs and b) including also installation costs

41m and 50m, with a step size of 30cm. R_{out} varies between 3.5m and 4.2m, with a step size of 7cm. Installation costs increase with larger R_{off} , penalising designs with larger footprints. Thus, the optimal design obtained while considering both fabrication and installation costs has a lower footprint area than the design that minimises only the fabrication costs. Note that designs that do not achieve sufficient hydrostatic restoring moment due to too small combinations of R_{off} and R_{out} have to compensate with a deeper draft or larger central column's radius, which causes a severe increase in fabrication costs. This is the cause of the steep cost increase shown in the bottom left corner of Figure 3 a) and c). Overall, optimising the design of the semi-submersible accounting for both fabrication and installation costs yields a total cost of 3.659M€ per floating unit, against 3.667M€ obtained when optimising the floater only to minimise manufacturing costs. Note that the number of significant digits in the cost figures is representative of the magnitude of the exchange between fabrication and installation costs, and not of the accuracy of the absolute cost figure. For this case study, accounting for this trade-off results in a cost reduction of only 0.23%, which can be regarded as small when compared with the uncertainty of the models involved in this analysis. However, this cost reduction is achieved with a substantial decrease of 9.3% of the footprint area of the semi-submersible.

A sensitivity analysis is performed on the area required to store the semi-submersibles at the shipyard. Two key parameters are varied: the number of floaters to be stored at the same time and the amount of area required for internal movements. In fact, the first substructures could be transported from the shipyard to the port before the conclusion of the fabrication process for all the floaters of the farm, or even manufactured and installed in different instances. This approach would reduce the number of substructures to be stored simultaneously. The determination of the optimal moment to start the transportation procedure is beyond the scope of this work. It is expected that this would require capturing delays due to mismatches between the manufacturing and installation pipelines that counteract the decrease in storage costs when the manufacturing and installation processes are executed in parallel. In this work, we assumed a perfect match between the manufacturing and installation pipelines. The choice of the 10% extra storage space to allow for internal movements was also arbitrary, and could vary depending on project requirements. The cases considered for the sensitivity analysis are reported in Table 4, together with the results obtained considering only manufacturing costs (BCMO) and those achieved with the initial assumption on space requirements at the shipyard (BCI). When the number of substructures to be stored decreases, the cost-saving yielded by reducing the storage space at the shipyard is outweighed by the increase in manufacturing costs due to the larger columns

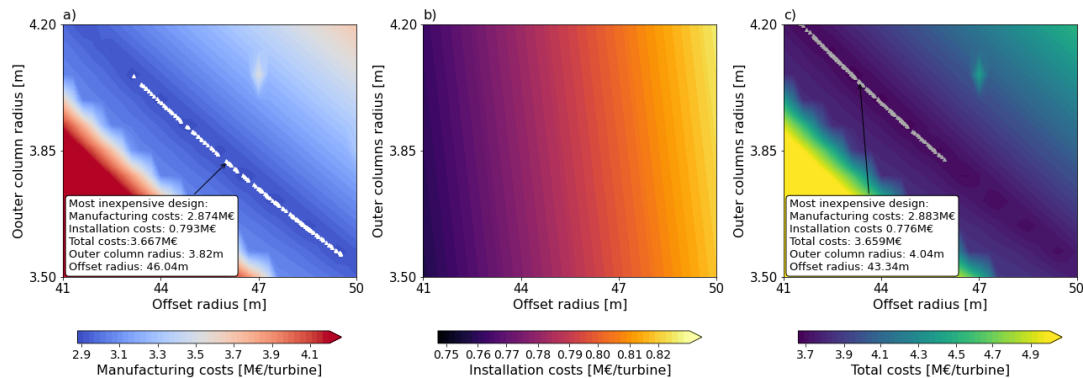


Figure 3. a) fabrication costs, b) installation costs and c) total costs obtained optimising the semi-submersible for different combinations of R_{off} and R_{out} , to minimise manufacturing costs. The most cost-effective designs individuated via multi-start optimisation are represented in a) as white triangles for the optimisation targeting only manufacturing costs, and in c) as grey triangles for the optimisation targeting both fabrication and installation costs

Table 4. Cases considered for sensitivity analysis on the area required to store the semi-submersibles at shipyard, resulting optimal R_{off} and R_{out} , and cost reduction obtained optimising the semi-submersible for both fabrication and installation costs

Case study	BCMO	S1	S2	S3	S4	BCI	S5	S6	S7
Units to be stored at the same time	none	6	10	15	30	all	all	all	all
Extra area to allow for internal movements	none	none	none	none	none	10%	40%	70%	100%
Offset radius [m]	46.04	45.73	45.72	45.39	44.75	43.34	42.79	42.26	41.74
Radius outer columns [m]	3.82	3.84	3.84	3.87	3.92	4.04	4.09	4.14	4.18
Cost reduction %	none	< 0.01	< 0.01	0.01	0.05	0.23	0.36	0.51	0.67

necessary to achieve stability with a lower footprint. In this case, the most cost-effective design approaches the optimum obtained by considering only fabrication costs, and the advantage of considering both manufacturing and installation costs in the design process becomes negligible. Contrarily, when the requirement for the storage area increases, the cost reduction achieved by coupling fabrication and installation costs grows up to 0.67% for the cases considered in this study. This is achieved with a 14.6% smaller footprint than for the fabrication-only case.

3.2. Sensitivity study

A further sensitivity study was carried out on key input parameters that were considered constant in the analysis performed in Section 3.1. Chiefly, this additional sensitivity was undertaken to understand the significance of the coupling between manufacturing costs and storage costs for different conditions than those considered in the initial case study and following sensitivity analysis on storage space. Secondly, this further sensitivity analysis indicates how varying key input parameters affects the most cost-effective design individuated. The parameters considered

for the sensitivity analysis are th_{clm} , MCF , and the workability factor. The sensitivity was carried out for all the different storage space requirements reported in Table 4, adopting the same multi-start approach. For the sensitivity to th_{clm} and MCF , the semi-submersible was also optimised for fabrication costs only. th_{clm} and MCF were varied of $\pm 20\%$ with respect to the case study reported in Section 3.1, while the workability factor was modified of $\pm 10\%$. Overall, the coupling effect remains important for all the cases considered, despite the variability in the resulting most cost-effective design driven by the variation of the key parameters object of the sensitivity study. As it is shown in Figures 4, 5, and 6 - b), c) and d) - when the requirement for storage space is small, the cost-optimal design approaches the one obtained by minimising fabrication costs only. Contrarily, larger storage area requirements make smaller footprints more cost-effective than in the fabrication-only case. In the latter case, higher cost savings can be achieved by optimising the structure while considering both installation and fabrication costs. This can be noticed in Figures 4, 5, and 6 - a).

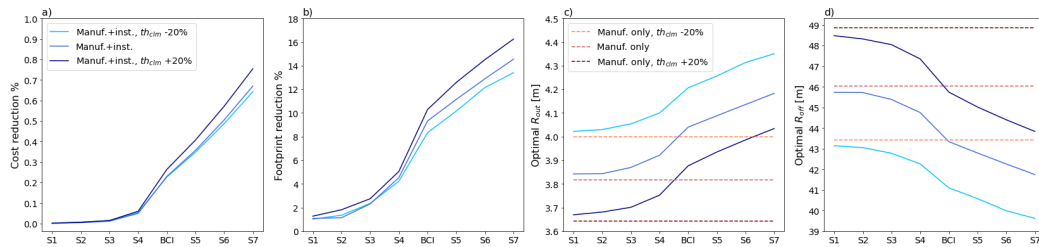


Figure 4. Sensitivity analysis on wall thickness. a) cost reduction and b) footprint reduction with respect to designs obtained minimising only fabrication costs. c) optimal R_{out} and d) optimal R_{off} obtained for all the cases reported in Table 4, considering both manufacturing and installation costs (solid lines), and for the manufacturing-only case (dashed lines)

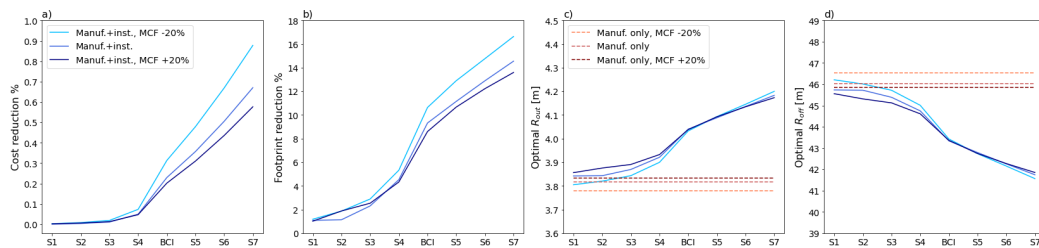


Figure 5. Sensitivity analysis on MCF . a) cost reduction and b) footprint reduction with respect to designs obtained minimising only fabrication costs. c) optimal R_{out} and d) optimal R_{off} obtained for all the cases reported in Table 4 considering both manufacturing and installation costs (solid lines), and for the manufacturing-only case (dashed lines)

Varying the wall thickness had a significant impact on the most cost-effective design obtained by minimising only manufacturing costs, as can be noticed in Figure 4 - c) and d). When wall thickness is decreased with respect to the initial case study, higher outer column and ballast costs are traded for lower costs of pontoons and cross braces. Reducing the wall thickness makes designs with larger R_{out} and lower R_{off} relatively more convenient, as increasing R_{out} leads to a lower increment in outer columns cost. Thus, a decrease of the wall thickness of 20% with respect to the case study introduced in Section 3.1 yielded a cost-optimal design with a 9.2% lower footprint for the fabrication-only case. The opposite occurs when wall thickness increases. Varying the MCF did not alter significantly the most cost-effective design obtained by

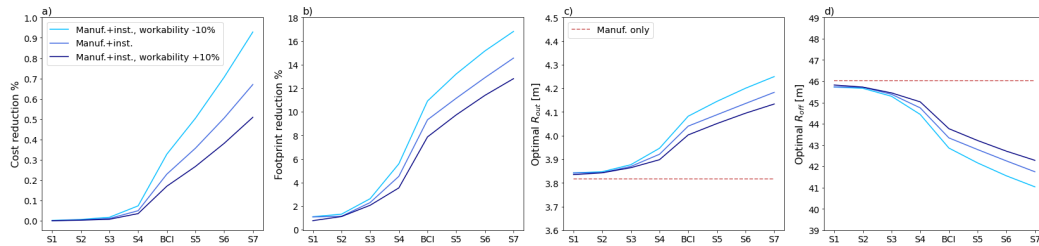


Figure 6. Sensitivity analysis on workability. a) cost reduction and b) footprint reduction with respect to designs obtained minimising only fabrication costs. c) optimal R_{out} and d) optimal R_{off} obtained for all the cases reported in Table 4 considering both manufacturing and installation costs (solid lines), and for the manufacturing-only case (dashed lines)

minimising fabrication costs only, as it is shown in Figure 5 - c) and d). Minimising the amount of steel in the structure remains the main driver for cost reductions in both the low and high MCF scenarios, yielding very similar designs to the initial case study. Lowering the MCF yielded a slightly larger R_{off} and slightly lower R_{out} for the fabrication-only case than the one obtained in the case study in Section 3.1. In this case, increased pontoons and cross braces costs are traded for lower outer columns and ballast costs, as cost-saving from ballast reduction becomes slightly more relevant. The opposite was observed with higher MCF .

The sensitivity to the workability is illustrated in Figure 6. When workability decreases with respect to the initial case study assumption, higher manufacturing costs are traded for lower storage costs to achieve a cheaper design. The contrary occurs when workability increases. The highest cost reduction with respect to the fabrication-only case, 0.93%, was achieved in the low workability scenario, corresponding to a footprint reduction of 16.8%.

4. Conclusions

We coupled an approach to size a semi-submersible while considering hydrostatic stability and a deterministic installation cost model inheriting from previous research works. This allowed to investigate the cost reduction potential of integrating fabrication and installation costs to design floating semi-submersibles for wind turbines. A trade-off between the fabrication costs and installation costs was identified, driven by the reduction of manufacturing costs obtained by increasing the structure's footprint and decreasing the outer columns' radius, which is counterbalanced by the increase in storage costs at the shipyard. For the case study, accounting for this trade-off yielded a design that is only 0.23% cheaper than optimising only the floater's fabrication costs, although the obtained design is significantly different from the fabrication-only case, having a 9.3% smaller footprint. The installation strategy has a significant impact on the trade-off. If the number of floaters to be stored simultaneously decreases, manufacturing costs outweigh storage costs. In this case, optimal designs are close to the manufacturing-only case, and coupling fabrication and installation costs yields negligible cost reductions. Instead, larger storage space requirements result in higher costs savings from a coupled approach. The trade-off remained important for all the cases considered in a further sensitivity study of key parameters affecting the most cost-effective design: wall thickness, manufacturing complexity factor and workability. Independently from the parameters' variation, the same trend highlighted in the initial sensitivity analysis on storage space was observed.

Several significantly different designs within a small cost range were identified. This suggests that further criteria could drive the best design choice, such as maximising the local contribution to the supply chain or minimising the operations and maintenance (O&M) costs.

Future work should point in two main directions. The first path should extend the scope of the

current workflow to account for missing wind farm elements, including moorings, electrical cable topology, layout definition and O&M. This extension would allow accounting for more couplings and ultimately identify the most important trades that can be exploited to reduce the LCoE of the whole wind farm. The second direction for future work should increase the models' fidelity to enable the use of the workflow in an engineering design environment. To this end, the next steps should be including a more detailed stability analysis and structural integrity verification.

Acknowledgements

This work is part of the STEP4WIND project (www.step4wind.eu) and has received funding from the European Union's Horizon 2020 research and innovation program under grant agreement No. 860737.

References

- [1] DNV GL 2020 *Floating wind: the power to commercialize*
- [2] Jiang Z 2021 *Renewable and Sustainable Energy Reviews* **139**
- [3] Hall M, Buckham B and Crawford C 2013 "Evolving offshore wind: A genetic algorithm-based support structure optimization framework for floating wind turbines," 2013 MTS/IEEE OCEANS Bergen
- [4] Karimi M, Hall M, Buckham B and Crawford C 2017 *J. Ocean Eng. Mar. Energy* **3** 69-87
- [5] Ioannou A, Liang Y, Jalón M L and Brennan F P 2020 *Ocean Engineering* **197**
- [6] Ghigo A, Cottura L, Caradonna R, Bracco G and Mattiazzo G 2020 *J. Mar. Sci. Eng.* **8** 835
- [7] Dou S, Pegalajar-Jurado A, Wang S, Bredmose H and Stolpe M 2020 *J. Phys.: Conf. Ser.* **1618** 042028
- [8] Leimeister M, Collu M and Kolios A 2020 *Preprint* wes-2020-93
- [9] Stehly T, Beiter P and Duffy P 2019 *2019 Cost of Wind Energy Review* National Renewable Energy Laboratory
- [10] Adam F, Ritschel U, Dahlhaus F and Grossmann J 2016 "Development of an economical and insured TLP substructure for a 6MW wind turbine - use of steel-concrete composite material," *Int. Conf. on Offshore Renewable Energy - CORE 2016* Glasgow
- [11] Borg M, Walkusch Jensen M, Urquhart S, Andersen M T, Thomsen J B and Stiesdal H 2020 *Energies* **13** 4911
- [12] Jonkman J, Butterfield S, Musial W and Scott G 2009 *Definition of a 5-MW Reference Wind Turbine for Offshore System Development*
- [13] Jonkman J 2010 *Definition of the Floating System for Phase IV of OC3*
- [14] Robertson A, Jonkman J and Masciola M 2014 *Definition of the Semisubmersible Floating System for Phase II of OC4*
- [15] Myhr A, Bjerkseter C, Ågotnes A, and Nygaard T A 2014 *Renewable Energy* **66** 714-728
- [16] NREL WISDEM Team 2019 *Theory — WISDEM 2.0 documentation* URL: <https://wisdem.readthedocs.io/en/latest/wisdem/floatingse/theory.html#pitch>
- [17] Leimeister M 2016 *Rational Upscaling and Modelling of a Semi-Submersible Floating Offshore Wind Turbine* MSc thesis
- [18] Gray J S, Hwang J T, Martins J R, Moore K T, and Naylor B A, 2019 *Structural and Multidisciplinary Optimization* **50** 1075–1104
- [19] Matha D, Brons-Illig C, Mitzlaff A, and Scheffler R 2017 *Energy Procedia* **137** 299-306
- [20] D3.1 COREWIND 2020 *D3.1 Review of the state of the art of dynamic cable system design*
- [21] Castro-Santos L, Filgueira-Vizoso A, Lamas-Galdo I and Carral-Couce L 2018 *Journal of Cleaner Production* **170** 1124-1135
- [22] Dewan A, Asgarpour M and Savenije R 2015 *Commercial Proof of Innovative Offshore Wind Installation Concepts using ECN Install Tool*
- [23] NREL 2020 *Moored Substructure Installation Methodology — ORBIT* URL: https://wisdem.github.io/ORBIT/source/phases/install/quayside_towout/doc_MooredSubInstallation.html
- [24] ORE Catapult 2020 *Floating wind: Cost modelling of major repair strategies*
- [25] Harrison J, Garrad A, Warren T, Powell J 2020 *Floating Offshore Wind: Installation, Operation & Maintenance Challenges*
- [26] Port of Cromarty Firth 2021 *Rates and Charges*
- [27] Forth Ports Limited 2021 *Marine rates and Charges*
- [28] Bjerkseter C and Ågotnes A 2013 *Levelised Costs of Energy for Offshore Floating Wind Turbine Concepts* MSc thesis